Complex Embedded Automotive Control Systems
CEmACS

DaimlerChrysler
SINTEF
Glasgow University
Hamilton Institute
Lund University

Public Integrated Chassis Control Controller Specification Deliverable D8

Carlos Villegas
Mehmet Akar
Robert Shorten

October 2005

Contents

.

1 General objectives

The specific objective of this work package is to provide controller specifications for the Integrated Chassis Controller (ICC). The basic task of the ICC is to enable the test vehicle, Pegasos, to emulate a range of reference vehicles. In particular, Pegasos will be used to emulate the dynamics of vehicles with a shorter wheel base than itself, of which the SMART automobile is an example.

Our basic strategy is to use a four wheel steering system to control the vehicle lateral dynamics (Side-slip, Yaw-rate), and to use the vehicle suspension to control the vehicle vertical dynamics (Roll-angle). Naturally, both subsystems affect each other and an integrated design is necessary if the degree of interaction is large. In addition, the control structure should account for actuator constraints and be robust to system uncertainties and external disturbances. The second major consideration in developing the basic control strategy is that the final control structure should be robust to the effects of actuator saturation and rear steering actuator failure, and to the effects of sensor failures.

This report presents the second milestone (MS2) of the work package WP2 and is structured as follows. We begin by describing the reference models that are used to generate the reference trajectories. We then use these reference models, and knowledge of the test vehicle actuator constraints, to estimate an emulation envelope of the test vehicle. This amounts to establishing the types of vehicles that can be emulated using Pegasos and consists of verifying, whether or not, a given set of maneuvers are consistent with the performance specifications for the test vehicle actuators. The final part of the report is concerned with the basic controller specifications for the emulation task.

2 Problem setup

The emulation capabilities of the test vehicles are determined by whether the test vehicle is able to follow a set of reference signals that are generated by reference maneuvers and reference dynamics. The reference dynamics are specified in terms of reference models for Yaw, Side-slip and roll-angle that have been supplied by DaimlerChryslerin [1].

2.1 Test and Reference Vehicles

The reference and test vehicles are SMART and Pegasos, respectively, the latter of which is described in Deliverable D11. The parameters which we use to determine the emulation envelope are summarized in Tables 1 and 2.

Physical parameter	value	unit
Mass (m)	868.7	kg
moment of inertia (I_{zz})	617	kg m^2
Front tire stiffness (C_f)	42058	N/rad
Rear tire stiffness (C_r)	122000	N/rad
Horizontal COG from front (l_f)	1.1029	m
Horizontal COG from rear (l_r)	0.7907	m
Steering transmission ratio (I_L)	25	-

Table 1: SMART parameters

Physical parameter	value	unit
Mass (m)	1448	kg
Moment of inertia (I_{zz})	1945.6	kg m^2
Front tire stiffness (C_f)	71380	N/rad
Rear tire stiffness (C_r)	134680	N/rad
Horizontal COG from front (l_f)	1.208	m
Horizontal COG from rear (l_r)	1.179	m
Steering transmission ratio (I_L)	19.8	-

Table 2: PEGASOS parameters

2.2 Reference Maneuver

Since we are interested in the emulation capabilities of Pegasos, we test with a worst case input that is designed by considering two key criteria: the driver, and the operating regime. A skillful driver can steer the wheel at a rate of 1000 degrees per second. However, the steering angle is limited to a maximum value so that the lateral acceleration is less than 4 m/s^2. Therefore, the worst case input is defined as the ramp input which has a slope of 1000 deg/s, and saturated at δ_{max} so that lateral acceleration of 4 m/s^2 is not exceeded in steady state. For example, Figure 3 depicts the SMART input with $\delta_{max} = 67.6$ (in degrees) for $v = 15$m/s.

2.3 Reference models

The reference dynamics are given by a set of reference models that have been specified by DaimlerChrysler in [1]. These are derived from a 4-state single track model with the steering wheel angle (δ_{sw}) as input and are:

(i) **Side-slip β:**

$$\dot{\beta} = \frac{-(C_r l_r - C_f l_f)\dot{\psi} - (C_f + C_r)v_x\beta}{m v_x^2} + \dot{\psi}v_x - \frac{C_f \delta_{sw}}{m I_L}, \tag{1}$$

(ii) **Yaw rate $\dot{\psi}$:**

$$\ddot{\psi} = \frac{-(C_r l_r - C_f l_f)v_x\beta - (C_f l_f^2 + C_h l_f^2)\dot{\psi}}{I_{zz} v_x} + \frac{C_f l_f \delta_{sw}}{I_{zz} I_L} \text{ and} \tag{2}$$

(iii) **Roll angle ϕ:**

$$\ddot{\phi} + 2\xi_w \omega_0 \dot{\phi} + \omega_0^2 \phi = \omega_0^2 R_\delta(v_x)\delta_{sw}. \tag{3}$$

The parameters of the the reference models are defined in Table 1 together with $\zeta_w = 0.6$, $\omega_0 = 6.6 rad/s$ and $R(v_x)$ being a speed dependent gain (see Equation (10) in Section 4).

2.4 Vehicle emulation envelope

The test vehicle to be used for the emulation task is Pegasos. Pegasos is documented in Deliverable 11 (D11). A basic strategy to determine whether Pegasos can emulate a given vehicle is as follows. The reference signals are fed into a one-track model inverse of Pegasos. The emulation capability of Pegasos is determined by observing whether the suspension/steering actuator limits are exceeded for the given reference maneuver.

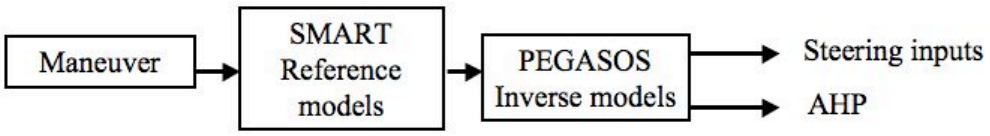

Figure 1: Emulation setup

3 Lateral Dynamics Emulation Envelope

In this section, we discuss the range of vehicles whose lateral dynamics can be emulated with Pegasos. Our experiments have indicated that the coupling from the vertical to the lateral is relatively weak. This observation allows us to consider the lateral dynamics independently.

	δ [deg]		$\dot{\delta}$ [deg/s]		$\ddot{\delta}$ [deg/s^2]	
	without load	with load	without load	with load	without load	with load
Front	700	700	1400	1000	100000	100000
Rear	5	5	150	150	10000	10000

Table 3: Actuator limits from DaimlerChrysler. The front steering values should be divided by the steering transmission ratio of 19.8

3.1 Actuator Constraints

The actuator specifications provided by DaimlerChryslerare given in Table 3 where the limits for up to the second derivatives of the steering angles. The values for the front are subject to the steering transmission ratio (I_L) which relates the steering wheel angle δ_{sw} and the steering angle at the tyres δ_f as follows

$$\delta_{sw} = I_L \delta_f \tag{4}$$

On the other hand, the actuator limits for the rear are associated directly to the rear steering angle at the tyre δ_r.

The measurements for the unloaded car are obtained by lifting the wheels up; therefore, the limits for the loaded case are considered to determine the emulation envelope.

3.2 Models

The reference model and the test vehicle model are both based on the one-track model. The latter is a linear model that assumes both tyres at front (rear) axle to be replaced by one imaginary tyre at the axle geometrical center. Front and rear imaginary tyres are joined together with an imaginary weightless rod. While mass is concentrated at a point between the front and rear axle in the simple one-track model, when roll is considered, it is assumed to be above the weightless rod and rotating about it. The models are valid on high friction roads below 0.4g (approximately 4m/s^2).

The one track bicycle model

$$\dot{x} = Ax + Bu, \tag{5}$$

where

$$x = [\beta, \dot{\psi}]^T,\ u = [\delta_f, \delta_r]^T, \tag{6}$$

$$A = \begin{bmatrix} -\frac{C_f + C_r}{m v_x} & \frac{C_f l_f - C_r l_r}{m v_x^2} + 1 \\ \frac{C_f l_f - C_r l_r}{I_{zz}} & -\frac{C_f l_f^2 + C_r l_r^2}{I_{zz} v_x} \end{bmatrix} \text{ and } B = \begin{bmatrix} -\frac{C_f}{m v_x} & -\frac{C_r}{m v_x} \\ \frac{C_f l_f}{I_{zz}} & -\frac{C_f l_f}{I_{zz}} \end{bmatrix}, \tag{7}$$

denote the Pegasos with the system matrices (A_p, B_p) in (7) by substituting the values in Table 2. Similarly, the SMART matrices are (A_s, B_s) by substituting the values in Table 1. However, for SMART there is no rear steering input, i.e., $\delta_r = 0$; therefore B_s is the first column of B with values substituted from Table 1.

3.3 Emulation Setup

The worst case input described above is fed to the reference model to generate the reference signals to be tracked. These reference signals are then used in the inverse Pegasos model as shown in Figure 2 to determine the steering angles required and to see if actuator constraints are violated.

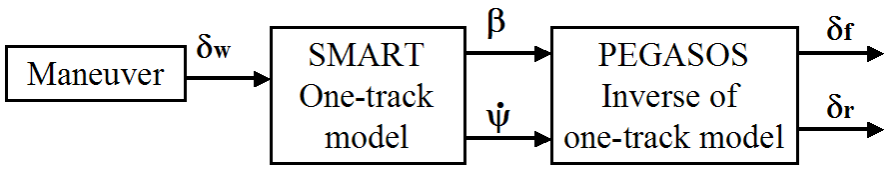

Figure 2: Test Structure

3.4 Lateral Emulation Envelope

Simulation Result 1:

We first perform tests to determine whether Smart can be emulated. The experiments are done at three different velocities: 15, 25, and 35m/s. For $v = 15$m/s, the input in Fig. 3 generates the lateral acceleration in Fig. 4.

The steering input required for Pegasos are depicted in Figs. 5–7. Although the constraints for δ_f, δ_r, $\ddot{\delta}_f$ and $\ddot{\delta}_r$ are satisfied (Figs. 5 and 7, respectively), the constraint for $\dot{\delta}_f$ is violated (see Fig.6). Similar simulation conclusions hold for $v = 25m/s$ and $v = 35m/s$.

Simulation Result 2: In this case we simulate Smart with additional mass which may arise due to additional passengers and load. We assume that the moment of inertia varies according to

$$I_{zz} = 617 + \Delta m l^2, \tag{8}$$

where Δm is the additional mass, and l is the distance to the center of gravity which is assumed to be $l = 0.25$ meters. The simulation results are summarized in Table 4 from which we note that the Smart vehicle with additional loading can be emulated by Pegasos.

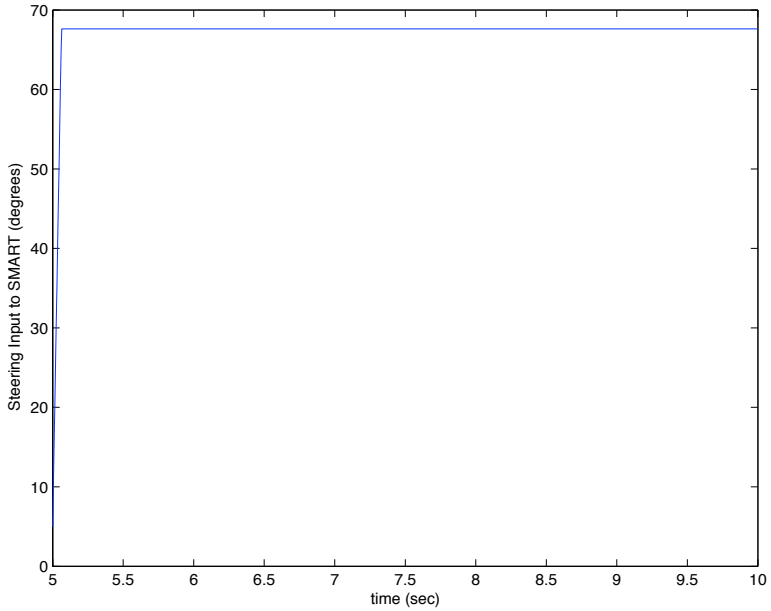

Figure 3: Worst case input for Smart (v=15m/s)

Velocity (v)	15 m/s	25 m/s	35 m/s
Additional mass (Δm)	$\geq$ 130.3 kg	$\geq$ 139 kg	$\geq$ 139 kg
Percentage of nominal mass	$\geq \%15 m_s$	$\geq \%16 m_s$	$\geq \%16 m_s$

Table 4: Additional loading required in Smart so that it can be emulated by Pegasos

Simulation Result 3:

In this part, we determine the range of parameters m, I_{zz}, C_v, C_h, l_f, and l_r so that, when varied independently, the modified Smart can be emulated by Pegasos. The results are summarized in Table 5.

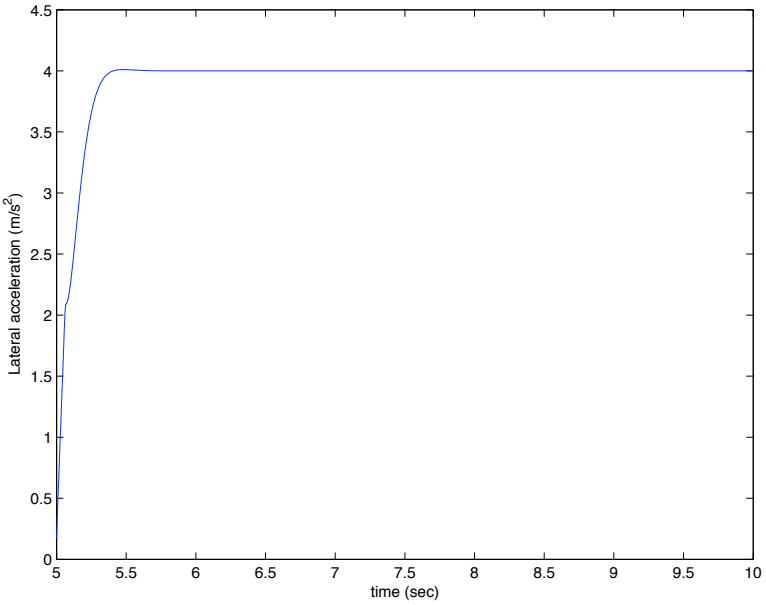

Figure 4: Lateral acceleration (v=15m/s)

Simulation Result 4:

In Simulation Result 1, we have determined that SMART can not be emulated by Pegasos for the worst case steering input which has a slope of 1000 deg/s. However, as seen in Table 6, the emulation may be feasible by reducing the value of the slope of the steering input.

4 Vertical dynamics envelope

4.1 Roll reference model

The reference model relates the roll angle ϕ and the steering wheel angle δ_{sw}, and is described by the second order transfer function

$$\phi = \frac{R_\delta(v_x)}{s^2/\omega_0^2 + 2\xi_w/\omega_0 s + 1}\delta_{sw}, \tag{9}$$

where ϕ is the roll angle (in degrees), $R_\delta(v_x)$ is the roll stiffness, ω_0 is the natural frequency (in rad/s) and ξ_w is the damping coefficient. The roll stiffness $R_\delta(v_x)$ is assumed to be linear in velocity and described by

$$R_\delta(v_x) = R_0 + m_0 v_x, \tag{10}$$

where v_x is the velocity (in m/s), and the parameters R_0 and m_0 are constants that were obtained from the initial data provided by DaimlerChrysler(verbal communication from Jens Kalkkuhl) and are presented in Table 7.

Velocity (v)	15 m/s	25 m/s	35 m/s
Mass (m)	≥ 1025.1 ($\geq$ %118)	≥ 1033.8 ($\geq$ %119)	≥ 1033.8 ($\geq$ %119)
Moment of inertia (I_{zz})	≥ 678.7 ($\geq$ %110)	≥ 678.7 ($\geq$ %110)	≥ 678.7 ($\geq$ %110)
Horizontal COG from front (l_f)	≤ 0.9926 ($\leq$ %90)	≤ 0.9926 ($\leq$ %90)	≤ 0.9926 ($\leq$ %90)
Horizontal COG from rear (l_r)	≥ 1.7372 ($\geq$ %245)	≥ 2.1059 ($\geq$ %297)	≥ 2.403 ($\geq$ %339)
Front tire stiffness (C_f)	≤ 39535 ($\leq$ %94)	≤ 39535 ($\leq$ %94)	≤ 39535 ($\leq$ %94)
Rear tire stiffness (C_r)	$\in [31720, 35380]$ (%[26, 29])	$\in [47580, 51240]$ (%[39, 42])	$\in [53680, 59780]$ (%[44, 49])

Table 5: Vehicle emulation envelope

Velocity (v)	15 m/s	25 m/s	35 m/s
Maximum slope	948.7	945.1	943.5

Table 6: Maximum slope values for the input so that SMART can be emulated by Pegasos

Paramter	Value	Unit
ω_0	$2\pi 1.05$	rad/s
ξ_w	.6	-
R_0	-.018	-
m_0	.003	s/m

Table 7: Roll reference model parameters

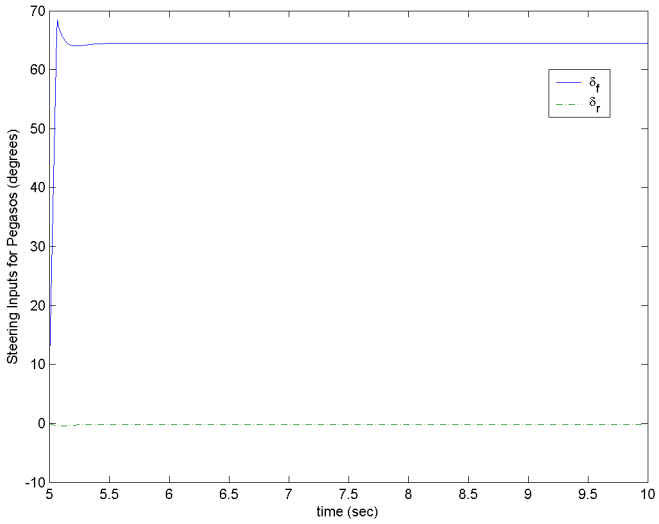

Figure 5: Pegasos steering inputs at v=15m/s

	suspension displacement	in m	suspension velocity	in m/s
	min	max	min	max
Front	-0.0856	0.0856	-0.18	0.18
Rear	-0.0856	0.0856	-0.18	0.18

Table 8: Actuator limits from DaimlerChrysler.

4.2 Suspension Actuator Constraints

The actuator system used in the suspension of the test vehicle Pegasos is described in D11. The specifications provided by DaimlerChryslerare in Table 8. The maximum displacement of the actuators is equivalent to that of the suspension strut for this suspension type and the maximum velocity was obtained using the current suspension controller.

4.3 Emulation envelope of suspension system

Simulation Result 1:

Let us now repeat the first experiment performed for lateral dynamics to see if the vertical emulation holds. The procedure is to use the reference model with the steering wheel maneuver described in section 2.2 as an input. The outputs of the reference model are the roll angle and the roll angular velocity. The maximum values are depicted in the Table 9 for 15, 25 and 35 m/s.

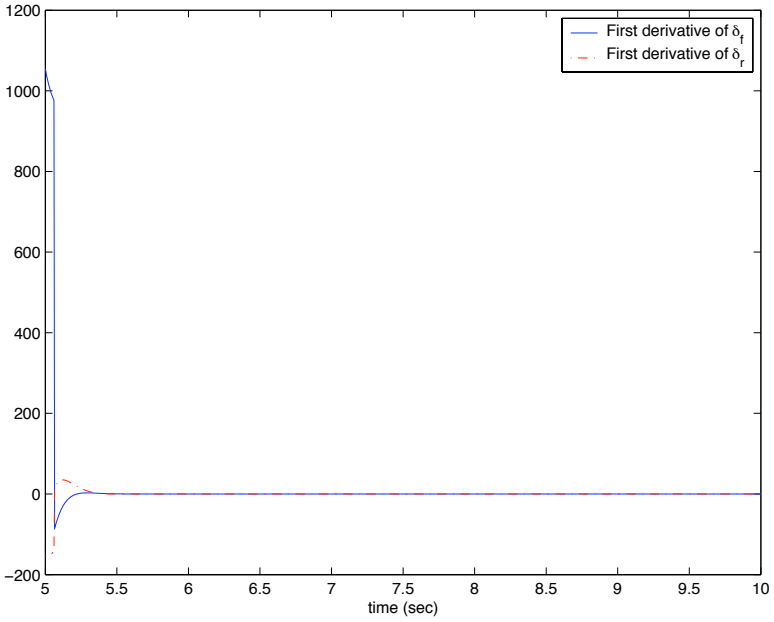

Figure 6: First derivative of Pegasos steering inputs at v=15m/s

Velocity in m/s	Maximum roll in degrees	Maximum roll velocity in deg/s
15	2.211	6.603
25	2.826	8.491
35	3.539	10.643

Table 9:

These values can be directly used to establish whether the vertical dynamics can be emulated by considering the roll angle to be proportional to the struts vertical displacement defined by

$$\tan\phi = \frac{z_{SSleft} - z_{SSright}}{2t} \tag{11}$$

where z_{SSleft} and $z_{SSright}$ are the strut vertical displacements and t is the half–track width which is equal to 0.88 m. Assuming small angles and that there is no heave motion (i.e., the roll axis is not displaced vertically) we can rewrite the suspension displacement z_{SS} and its derivative as

$$z_{SS} = t\phi \text{ and} \tag{12}$$
$$\dot{z}_{SS} = t\dot{\phi}. \tag{13}$$

The results in Table 10 were obtained by making use of the previous equation to

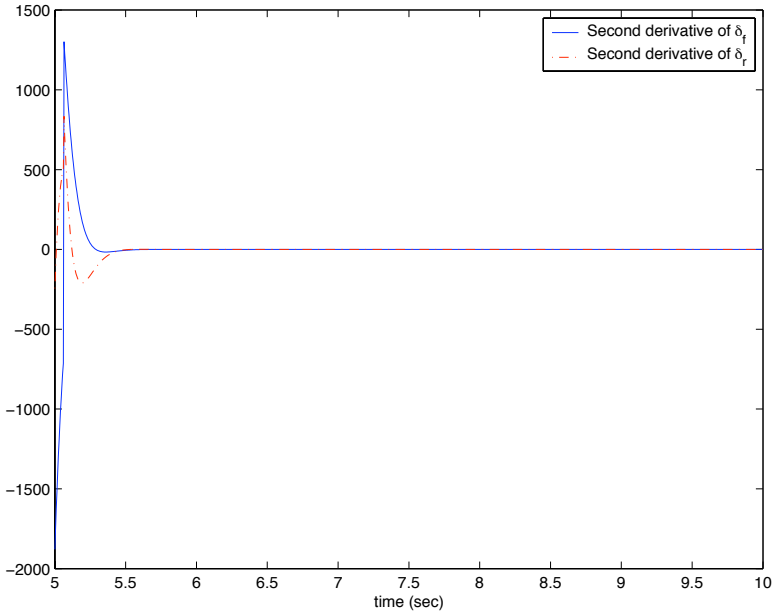

Figure 7: Second derivative of Pegasos steering inputs at v=15m/s

Velocity	Max. Susp. displacement [cm]		Max. Susp. velocity [m/s]	
	Front	Rear	Front	Rear
15	3.31	3.48	0.0988	0.1041
25	4.23	4.45	0.127	0.1338
35	5.29	5.58	0.1592	0.1677

Table 10:

calculate the maximum displacement and velocity required by the suspension in order to perform the emulation. The max. required displacement are for all velocities below the maximum actuator displacement of 8.56cm and maximum velocity of 0.18 m/s although for a vehicle longitudinal speed of 35 m/s the rear actuator is close to the displacement rate limits.

Simulation Result 2:

Let us now come back to Simulation result 4 for the lateral dynamics. It was noticed that the vehicle SMART could not be emulated for a maneuver with a slope of 1000 deg/s. As a result, maximum slopes were calculated for different velocities. The same experiment was conducted for vertical dynamics to show that the vehicle was also emulatable for these less stringent conditions. The results are given in Table 11.

Velocity m/s	Maneuver Slope deg/s	Max. Susp. displ. (cm) Front	Rear	Max. Susp. Vel. (m/s) Front	Rear
15	948.7	3.31	3.48	0.0987	0.104
25	945.1	4.23	4.45	0.1269	0.1338
35	943.5	5.29	5.58	0.1591	0.1677

Table 11:

4.4 Discussion: Models of the AHP

The new test vehicle Pegasos is fitted with an active suspension system called Active Hydropneumatic (AHP). As opposed to conventional suspensions, a hydraulic valve replaces the mechanical damper and a hydropneumatic accumulator (containing both hydraulic fluid and gas) replaces the mechanical spring in AHP. A full description of this suspension model can be found in [2] and a simpler version in [3], [4] and [5].

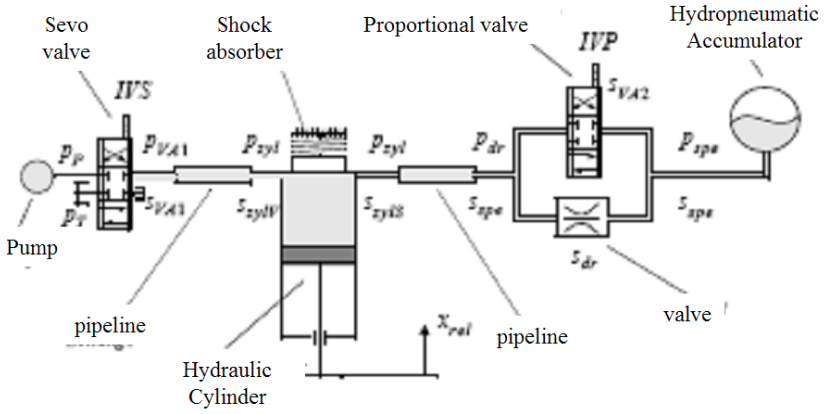

Figure 8: Active Hydropneumatic Suspension graphic representation [2]

In Deliverable 2, a model for the vertical dynamics was developed for the test car Technoshuttle. That model accounted for a test vehicle with an active suspension of the type using mechanical springs and dampers, and therefore has to be modified to account for the AHP.

Recall from D2 that the vertical dynamics of the chassis (heave z_s, pitch z_θ and roll z_ϕ) are functions of the suspension strut forces F_{ss} and the accelerations acting at the center of gravity (lateral a_y and longitudinal a_x):

$$m_s \ddot{z}_s = -\sum_{i=1}^{4} (r_{Di} F_{ssi}) , \tag{14}$$

$$I_\theta \ddot{z}_\theta = \sum_{i=1}^{4} (r_{xi} r_{Di} F_{ssi}) - m_s h_p a_x \text{ and} \tag{15}$$

$$I_\phi \ddot{z_\phi} = \sum_{i=1}^{4} ([(1 - r_{Di})r_{Bi} - r_{ssi}F_{ssi}]) + m_s h_r \left(\dot{v}_y + \dot{\Psi} v_x\right), \quad (16)$$

where i stands for every tyre of the car (front-left, front-right, rear-left, rear-right). The vertical dynamics of the tyres z_{ui} are functions of the suspension strut forces F_{ss} and the tyre relative displacement from the road $(z_{ui} - z_{ri})$:

$$m_i \ddot{z}_{u_i} = r_{Di}F_{ssi} + k_{ti}(z_{ri} - z_{ui}). \quad (17)$$

From Figure 8 it is noted that the suspension cylinder occupies the suspension strut entirely. Neglecting the friction, the suspension strut force F_{ss} is equal to the inner area of the cylinder A_{cyl} times the pressure at the cylinder, i.e.,

$$F_{ss} = A_{cyl}p_{cyl}. \quad (18)$$

As a first step, we did experiments to verify the applicability of the relatively complex model described in [2]. More specifically, the test vehicle and the model in [2] were applied an electrical current (i_{ci}) frequency sweep and the cylinder pressure was measured.

Figure 9 depicts a typical transfer function obtained from real data (car) and the supplied model. There is a considerable discrepancy between the curves for the model and the test vehicle at the low frequencies of interest. This may be simply due to the use of incorrect parameters for the model (parameters taken from [2]). Furthermore, the AHP has not been commissioned properly yet: therefore it does not reach its performance potential. Nevertheless, since we lack a systematic way of determining what the parameters should be or commissioning the AHP, alternative modelling methods which employ curve fitting, and other reduced order models in the literature, have been pursued.

For the purpose of compiling this report two approaches were followed to overcome these difficulties. Firstly, we used input-outut data to model the AHP. This gave the following first order transfer function for the AHP

$$p_{cyl} = \frac{1.0735 i_{ci}}{s + 0.4513}, \quad (19)$$

which approximates the data plotted in Figure 9 (dotted plot).

A second approach we have followed is to employ a simple linearised physical model from Yamashita and his co-workers [4]. This model described the dynamics of the AHP about a pressure operating point and relates suspension strut relative displacement $(z_{si} - z_{ui})$ and its derivative, the hydraulic flow from the servovalve (q_i) and its integral, and the electrical current input i_{ci}:

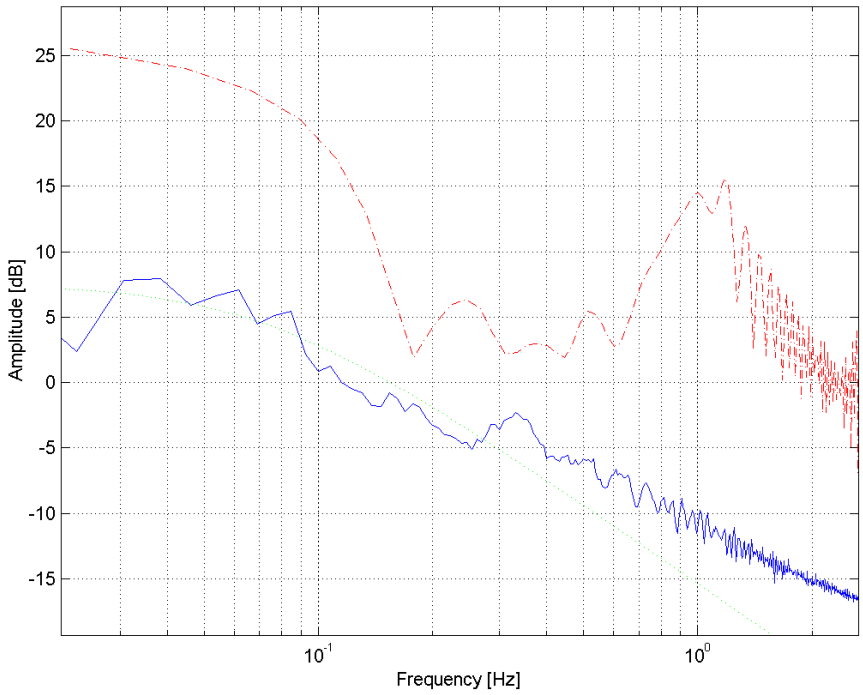

Figure 9: (continuous line) Experimental results, (-.-.) Simulation results and (....) first order approximation

$$p_{cyl} = C_{di}A_{cyl_i}\left(\dot{z}_{si} - \dot{z}_{ui}\right) + K_{gi}A_{cyl_i}\left(z_{si} - z_{ui}\right) + C_{di}q_i + K_{gi}\int q_i d\tau, \tag{20}$$

where A_{cyl_i} represents the inner area of the pistons, C_{di} the damping coefficient of the damping valves and K_{gi} the stiffness of the gas springs or accumulator. The dynamics of the flow rates from the servo valves to the cylinders (q_i) and their integrals ($v_{ci} = \int q_i d\tau$) are those of the electrovalve or servovalve. These dynamics can be modelled as [4]:

$$T_{Li}\dot{q}_i = -q_i + K_{vi}i_{ci} \text{ and} \tag{21}$$

$$\dot{v_{ci}} = q_i, \tag{22}$$

where T_{Li} and K_{vi} are the time constant and the flow rate coefficient of the servo valves, respectively.

Currenly, both models are being validated experimentally.

5 Basic controller specifications

The basic objective of the Integrated Chassis Controller is to enable Pegasos to emulate a range of target vehicles. In particular, Pegasos will be used to emulate the dynamics of vehicles with a shorter wheel base than its own, of which SMART is an example. Such emulation tasks are very difficult; consequently, a SMART vehicle will be used as an example and for project demonstration purposes. The specific objectives of the control system design can therefore be summarised as follows.

(i) Track Sideslip, Roll and Yaw-rate reference signals with a bandwidth that is as close as possible to that of the specified reference model. Table 12 gives the bandwidths of the reference models for the lateral dynamics.

(ii) Zero steady state error with respect to constant disturbances. Rejection of any disturbances in Sideslip, Roll and Yaw- rate by utilising the highest possible closed loop bandwidth.

(iii) Maintain tracking and disturbance rejection performance for a given set of reference manoevers for vehicle speeds between 15 and 35 m/s.

(iv) Robustness with respect to parameter uncertainty. Specifically, we hope to employ ICAD and techniques from SISO design for each control loop (Yaw, Sideslip, Roll). In this context, where possible, gain-margins of 8 to 10 $[dB]$ and phase margins of 30 $[deg]$ across a range of operating conditions will be required.

(v) Satisfactory performance (graceful degradation) with respect to actuator saturation; in particular with respect to rear steering actuator locking.

(vi) Graceful degradation of performance with respect to failure of feedback communication paths; namely, each control loop should contain a feed- forward component.

5.1 Reference models

Second order reference models for Yaw-rate, Slip and Roll are defined in [1] (see also Table 12 for details of the Yaw and Sideslip characteristic polynomials). Accurate parameters for the SMART roll model have yet to be determined by DaimlerChrysler and will be presented at the review meeting.

The specified bandwidths represent target bandwidths for each of the closed loops. The task of the control design is to emulate SMART: consequently, a basic requirement of the closed loop system is to achieve a bandwidth that is close to that of the reference models at each of the reference speeds.

Speed	ω_o rad/s	ζ
15 m/s	21.79	40.71
25 m/s	18.22	24.42
35 m/s	17.10	17.44

Table 12: Natural frequency and damping coefficients for second order Yaw and Side-Slip reference models.

5.2 Actuators

The following actuator information was supplied directly by Daimler Chrysler [1]. They specify the actuator limits for PEGASOS. Along with the reference models and reference maneuvers, these provide a basis for determining a range of vehicles that can be emulated using Pegasos. In addition, the actuator delays, along with the specified robustness margins, determine the actual achievable closed loop bandwidths.

Lateral dynamics

The front and rear steering actuator dynamics of Pegasos are assumed to behave as second order systems with the following transfer function:

$$\delta_i = \frac{1}{T_i^2 s^2 + \zeta_i T_i s + 1} u_i, \tag{23}$$

being u_i the steering angle of the tyres, δ_i the desired steering angle, T_i a time constant, ζ_i a damping constant and i stands for the front or rear. Empirical values for the actuator parameters were determined in [6] and are repeated in Table 13.

	$T_i[s]$	ζ_i
Front actuator	0.012	0.612
Rear actuator	0.0072	0.612

Table 13: Actuator dynamics from [6]

AHP suspension system

The AHP constraints are given in Table 16.

5.3 Disturbances

Lateral dynamics : The main disturbances affecting the lateral dynamics are

Front steering actuator	With load	Without load
Time delay [s]	0.007	0.007
Saturation [deg]	700	700
Rate constraints [deg/s]	1400	1000
Maximum acceleration [deg/s^2]	100000	100000
Bandwidth [Hz]	7	7

Table 14: Front steering actuator constraints. Steering transmission ratio 19.8:1

	With load	Without load
Time delay [s]	0.001	0.001
Saturation [deg]	$\pm$ 5	$\pm$ 5
Rate constraints [deg/s]	150	150
Maximum acceleration [deg/s^2]	10000	10000
Bandwidth [Hz]	7	7

Table 15: Rear steering actuator constraints.

disturbances from road inclination and road friction. Both disturbances are low frequency and must be dealt with by integral action in the control system. Initial tests have also indicated that for lateral accelerations below 4 m/s^2, the suspension system has little influence on the lateral dynamics. Consequently, we assume that below this limit the influence of the suspension system on the lateral dyanmics can be neglected and the lateral dynamics control design can be carried independently.

Vertical dynamics : The main objective of the suspension system will be to provide isolation from road disturbances and road irregularities and to track the roll angle reference signals. We will attempt to emulate the design advocated by Smith & Wang [7], and by Williams [8], and achieve both of these objectives simultaneously. Specifically, the objective will be to provide isolation from road irregularity below 5 Hz. Attention will be paid to the significant coupling from the lateral dynamics subsystem in the design of the roll tracking control system.

5.4 Robustness with respect to parameter uncertainties and subsystem failures

Both the lateral control system and the control system to follow reference roll trajectories will be designed to operate satisfactorily under empty and full load conditions as well as varying load distributions. In addition, we will assume a 10% uncertainty in relevant vehicle parameters (see Table 2) and require that the vehicle operate satisfactorily in this uncertainty band.

Several robustness issues arise in ICC design. Apart from conventional robustness

	With load	Without load
Time delay	0.0025 [sec]	0.0025 [sec]
Rate constraints	> 0.18 [m/s]	> 0.18 [m/s]

Table 16: AHP: Suspension (Initial measurements)

concerns stemming from parameter uncertainty, and uncertainty with respect to system delays, safety is a major consideration in steer-by-wire systems. Consequently, a major issue in the design of such systems is the effect of actuator locking and actuator failure as well as the effect of sensor failure. For both the vertical controller and the lateral controller, control designs will be developped that are robust to actuator /sensor failure and actuator locking. Moreover, gracefull degradation of performance in response to other forms of failure in the feedback paths will be partially addressed by requiring a feedforward component of both the lateral and vertical dynamics controller.

References

[1] F. Boettiger, "VFD synthetische modelle." DaimlerChrysler, July 1999.

[2] M. Rau, "Modellierung, simulation und auslegung eines hydropneumatischen federbeins mit schnell verstellbarer dämpfung," diplomarbeit, Universität Stuttgart, 2001.

[3] D. Hrovat, "Survey of advanced suspension developments and related optimal control applications," *Automatica*, vol. 33, no. 10, pp. 1781–1817, 1997.

[4] M. Yamashita, K. Fujimori, K. Hayakawa, and H. Kimura, "Application of H_∞ control to active suspension systems," *Automatica*, vol. 30, no. 11, pp. 1717–1729, 1994.

[5] P. A. Hoang Duong Tuan, Eichi Ono and S. Hosoe, "Nonlinear H_∞ control for an integrated suspension system via parameterized linear matrix inequality characterizations," *IEEE Transactions on Control Systems Technology*, vol. 9, Jan. 2001.

[6] N. Lazic, "Optimal vehicle dynamics - Yaw Rate and Side-slip angle control using 4-wheel steering," Master's thesis, Lund Institute of Technology, Oct. 2002.

[7] M. Smith and F. Wang, "Controller parameterization for disturbance response decoupling: application to vehicle active suspension control," *IEEE Transactions on Control Systems Technology*, vol. 10, May 2002.

[8] R. Williams and A. Best, "Control of a low frequency active suspension," in *Control '94 Conference IEE*, pp. 338–342, Mar. 2004. Publication No.389.